Proceeding of the IEEE
International Conference on Robotics and Biomimetics
Dali, China, December 2019

Research on Impedance Control of Flexible Joint Space Manipulator On-Orbit Servicing

Dongyu Liu [1,2], Hong Liu [2], Yechao Liu [2] and Zhiqi Li [2]

1. Institute of Manned Spacecraft System Engineering
China Academy of Space Technology
Beijing , China
liudongyu2004@126.com

2. State Key Laboratory of Robotics and System
Harbin Institute of Technology
Harbin , Heilongjiang Province, China
hong.liu@hit.edu.cn

***Abstract* - In this paper, the positional accuracy and contact force index requirements of the manipulator are analyzed according to the tolerance index of the space manipulator screwing. An position-based in Cartesian space impedance control strategy based on friction identification and compensation is proposed. By using joint friction torque compensation to improve the system control precision and setting the desired Cartesian position of the manipulator end point to control the contact force, this strategy solves the contradiction between the positional accuracy index and the contact force index requirement of manipulator during contact operating. The control algorithm is designed based on the system dynamics model, and the stability analysis of the control algorithm is given. The correctness of the control strategy is verified by simulation and on-orbit implementation. China's space manipulator has successfully completed the actual on-orbit servicing mission based on impedance control for the first time.**

Index Terms – space manipulator, on-orbit servicing, impedance control, flexible joint.

I. INTRODUCTION

The space manipulator generally has the characteristics of high load/self-weight ratio and large operating space. In order to improve the output efficiency of the joint, the joint generally uses a harmonic reducer as the transmission mechanism. To sense external loads, the joint also integrates a torque sensor. The addition of harmonic reducer and joint torque sensor will inevitably make the friction inside the joint complex and increase the flexibility, which will increase the difficulty of system control. In particular, the manipulator will inevitably come into contact with the environment when performing complex operations such as on-orbit maintenance and on-orbit assembly. The main problem is the contradiction between compliance (controllable contact force) with any environment in the contact operation task and high positioning accuracy in the free space transfer/positioning task.

Hogan systematically expounded the concept of impedance control in 1985 and proposed an impedance control strategy based on the dynamic model of the manipulator [1]. Impedance control does not directly control the desired position and the desired force, but by adjusting the dynamic relationship between the contact force and position of the manipulator to achieve the active compliance of the manipulator to the environment operated, and easy to achieve smooth transition between free space operation and restrained space operation. For joint torque-based manipulator, the traditional Cartesian impedance control strategy based on position and force does not perform well. Based on the passive control method [2][3], C.Ott and A.Albu-Schaeffer conduct in-depth research and extensive experimental analysis on flexible joint manipulators with joint torque feedback. However, there is no study on the nonlinear friction that widely exists in joints. Instead, it relies on parameters adjustment to reduce the influence of friction. Chen proposed an impedance control with adaptive friction compensation for the dexterous robot hand. When the friction model and parameters of the joint are not easy to be determined by the friction identification, the friction observer based on the extended Kalman filter is used to realize the adaptive observation and compensation of the friction force to achieve adaptive impedance control of dexterous hand fingers [4]. This method is a good solution for the nonlinear friction model and the difficulty of parameters calibration.

The researchers have conducted a large number of on-orbit experiments on the impedance control of space manipulators. DLR took the lead in implementing the on-orbit impedance control experiment in ROKVISS and conducted an experimental study on joint parameters [5]. NASA's Robonaut 2 applied a compliance control experiment based on joint torque sensor on the International Space Station. The operation included pressing buttons, plugging and unplugging connectors [6]. JAXA's ETS-VII uses impedance control on-orbit to perform a shaft hole assembly test [7]. At present, the research on impedance control of space manipulators in China is very extensive [8][9], but the application on-orbit has not been reported.

In order to verify the characteristics of the impedance control strategy in the contact operation of the flexible space manipulator, the Space Laboratory was equipped with a manipulator system, and arranged a manipulator screwing experiment during manned spacecraft Shenzhou - 11 berthing at the Space Laboratory Tiangong-2. Before the experiment, the on-orbit friction identification of the modular joint of the manipulator was first carried out, the friction model and parameters of the joint in the space environment were fully grasped [10]. Based on on-orbit friction identification, this paper proposes a flexible joint manipulator impedance control strategy with friction compensation. The practical operation of space manipulator based on impedance control is implemented in China for the first time. The successful implementation of the experiment has also accumulated certain experience for China's space manipulator to complete the contact operations.

978-1-7281-6321-5/19//$31.00 ©2019 IEEE

II. Mission Analysis

A. System Configuration

Experiment system is equipped with a manipulator with 6 degrees of freedom, a dexterous hand, a controller, global cameras, an orbit replaceable unit(ORU), a power tool, as shown in Fig. 1. ORU is fixed on the workbench with 2 bolts.

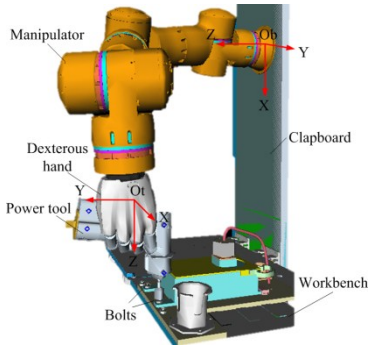

Fig. 1 Manipulator system screwing.

The joints are designed with the idea of mechatronics integration, include alternating current permanent magnet synchronous motor(PMSM), harmonic drive, cross roller bearing and multi-sensor integration system, as shown in Fig. 2. The motor stator is connected with the input side of the joint, the rotor of the motor is connected with the output side of the joint through harmonic reducer. The output side of the joint is equipped with a one-dimensional torque sensor, which can measure the external torque about the direction of joint rotation. The motor side is equipped with a resolver to measure the angular position of the motor shaft. The output side of the joint is equipped with a optical encoder, which can measure the angular position of the output side of the joint.

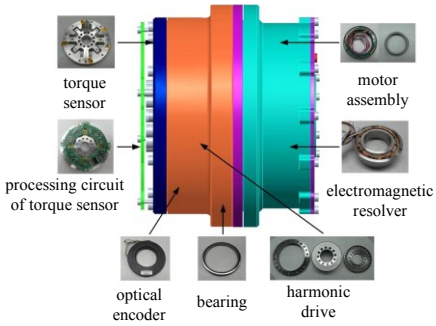

Fig. 2 Composition of modularized joint.

B. Analysis of Mission Tolerance and Control Index

After the manipulator grasps the power tool and positions the power tool above the bolt by visual servoing, when the manipulator is to control the power tool to insert the bolt, the relative position and orientation errors between the end of the power tool and the bolt is as shown in (1), including:

- Position and orientation errors of manipulator visual servoing control.
- Position and orientation errors caused by workbench deformation by the downward pressure of power tool.

$$\begin{cases} \Delta_T = \Delta_E + \Delta_S \\ \boldsymbol{\delta}_T = \boldsymbol{\delta}_E + \boldsymbol{\delta}_S \end{cases} \tag{1}$$

Where, $\Delta_T \in \mathbf{R}^3$ and $\boldsymbol{\delta}_T \in \mathbf{R}^3$ are respectively the relative position error and orientation error between the end of the power tool and bolt. $\Delta_S \in \mathbf{R}^3$ and $\boldsymbol{\delta}_S \in \mathbf{R}^3$ are respectively the position error and orientation error of the visual servoing control of the manipulator. The maximum position error of Δ_S in the three directions along the manipulator end coordinate system O_tXYZ does not exceed 0.7mm, the maximum orientation error of $\boldsymbol{\delta}_S$ in three directions around the coordinate system O_tXYZ does not exceed 1.0° [11]. $\Delta_E \in \mathbf{R}^3$ and $\boldsymbol{\delta}_E \in \mathbf{R}^3$ are the bolt position error and orientation error respectively due to the deformation of the workbench.

According to the the power tool and the bolt structure, under static working conditions the radial positioning tolerance of the power tool head to the bolt is 3 mm, the axial positioning tolerance is 3 mm, and the yaw/pitch direction attitude tolerance is 2 degrees. The necessary and sufficient condition for the success of the mission is (2):

$$\begin{cases} \max\{|\Delta_{Ex}|,|\Delta_{Ey}|,|\Delta_{Ez}|\} \le 2.3\text{mm} \\ \max\{|\boldsymbol{\delta}_{Ex}|,|\boldsymbol{\delta}_{Ey}|,|\boldsymbol{\delta}_{Ez}|\} \le 1° \end{cases} \tag{2}$$

By establishing a finite element model of the assembly of workbench and ORU, a 50N vertical downward force is applied to the bolt, and the maximum deformation of the workbench is simulated along the direction of the force, that is, the deformation amount in the Z direction of the coordinate system O_tXYZ is 2.66 mm, as shown in Fig. 3. The position of the bolt is about 500mm from the simplified fulcrum of the workbench, and the deformation around -Y direction is 0.3 degrees.

After the above analysis, the control indices of the screwing mission can be summarized into the following items:

- After visual servoing is aligned until the power tool contacts the bolt, control system no longer introduces other errors except elastic deformation of the workbench.
- After power tool contacts the screw, the force between manipulator (including the power tool) and the bolt does not exceed 40N.

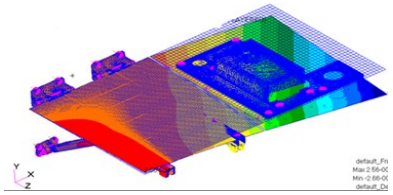

Fig. 3 Workbench deformation by pressure.

III. Dynamics Model of Flexible Joint Manipulator

In order to establish the flexible joint manipulator dynamics model which is convenient for the design of control strategy, the following reasonable assumptions are set :

Assumption 1: The motor rotor / reducer are symmetric about the rotor axis of rotation, and the rotation axis of the rotor / reducer is coaxial with the rotation axis of the joint.

Assumption 2: Compared to the dynamics of the joint mechanical system, it is considered that the joint electrical dynamics is fast enough, and the dynamics of the motor is not considered in the flexible joint model.

Assumption 3: The joint flexibility model is considered as a linear torsion spring between the motor rotor and the next link.

Assumption 4: The manipulator discussed in this paper works in a microgravity environment, and the influence of gravity is not considered in this paper, that is $g\left(q_i\right)\equiv 0$.

Assumption 5: The kinetic energy of the rotor of the joint motor is determined only by the speed of the rotor relative to the previous link. For the manipulator studied in this paper, the inertia of the rotor is much smaller than the inertia of the connecting link, and the reduction ratio is 160. Therefore, the kinetic energy of the rotor affected by the movement of the connecting link can be neglected.

The open-loop dynamics model of the flexible joint manipulator can be expressed as (3)~(5):

$$M\left(q\right)\ddot{q}+C\left(q,\dot{q}\right)\dot{q}+g\left(q\right)=\tau+\tau_{\text{ext}} \tag{3}$$

$$B\ddot{\theta}+\tau+\tau_f=\tau_{\text{m}} \tag{4}$$

$$\tau=K\left(\theta-q\right) \tag{5}$$

Where, $q=\left(q_1,\cdots,q_6\right)^T\in\mathbf{R}^{6\times 1}$ represents the angular position vector of the output side of the manipulator joint; $\theta=(\theta_1,\cdots,\theta_6)^T\in\mathbf{R}^{6\times 1}$ represents the angular position vector of the manipulator joint motor; $\tau=(\tau_1,\cdots,\tau_6)^T\in\mathbf{R}^{6\times 1}$ represents the joint torque vector; $\tau_{\text{ext}}=(\tau_{\text{ext1}},\cdots,\tau_{\text{ext6}})^T\in\mathbf{R}^{6\times 1}$ represents the external torque vector at the joint; $\tau_{\text{m}}=(\tau_{\text{m1}},\cdots,\tau_{\text{m6}})^T\in\mathbf{R}^{6\times 1}$ represents the electromagnetic drive torque vector of the joint motor; $\tau_f=\left(\tau_{f1},\cdots,\tau_{f6}\right)^T\in\mathbf{R}^{6\times 1}$ represents the joint friction torque vector converted to the joint motor side; $g\left(q\right)\in\mathbf{R}^{6\times 1}$ is a gravity vector, which can be ignored in the space microgravity environment; $M\left(q\right)\in\mathbf{R}^{6\times 6}$ is mass matrix of the rigid link of the manipulator; $B=\text{diag}(B_1,\cdots,B_6)\in\mathbf{R}^{6\times 6}$ is the diagonal matrix, which consists of the rotor inertias B_{i} ; $C\left(q,\dot{q}\right)\dot{q}\in\mathbf{R}^{6\times 1}$ represents the Coriolis force and the generalized centrifugal force matrix; $K=\text{diag}(K_1,\cdots,K_6)\in\mathbf{R}^{6\times 6}$ is the diagonal matrix formed by the joint stiffness K_{i} of the manipulator.

The relationship between the joint friction torque τ_f and joint motor angular velocity $\dot{\theta}$ is determined by joint friction identification on-orbit. According to the telemetry data of control input and joint angular velocity during experiments on orbit, the corresponding relationship between the viscous friction and the coulomb friction of the joints can be obtained [10]. In (6), $\hat{\tau}_f$ is the estimated value of the friction torque after identification; $\hat{d}$ is the estimated value of the viscous friction coefficient; $\hat{c}$ is the Coulomb friction coefficient.

$$\begin{cases}\hat{\tau}_f=\hat{d}\,\dot{\theta}+\hat{c} & \text{if: } \dot{\theta}\geq 0\\ \hat{\tau}_f=\hat{d}\,\dot{\theta}-\hat{c} & \text{if: } \dot{\theta}<0\end{cases} \tag{6}$$

IV. Control Strategy Design and Analysis

A. Impedance Controller Design

According to the proposed control missions for the section II. B. and the indices requirements, position-based in Cartesian space for impedance control (PB-CS-IC) scheme is adopted to realize the accurate positioning and stable control of the manipulator to insert the power tool into the bolt hole and screwing. Meanwhile, the scheme ensures that the force between the power tool and the bolt is controlled within the expected value. System block diagram is shown in Fig. 4.

By a negative feedback of the joint torque, the apparent inertia of the rotor can be scaled down[2]. The joint torque negative feedback expression is shown in (7).

$$\tau_{\text{m}}=BB_\theta^{-1}u+\left(I-BB_\theta^{-1}\right)\tau \tag{7}$$

Where, $B_\theta=\text{diag}(B_{\theta 1},\cdots,B_{\theta 6})\in\mathbf{R}^{6\times 6}$ represents the desired joint apparent inertia of manipulator; $I\in\mathbf{R}^{6\times 6}$ is an identity matrix; $u\in\mathbf{R}^{6\times 1}$ represents the new control input vector after joint torque feedback.

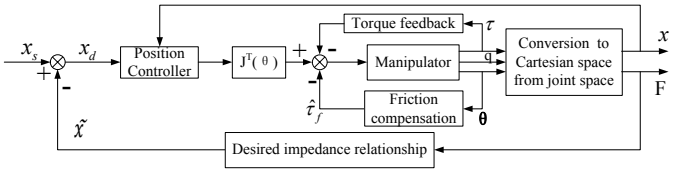

Fig. 4 System block diagram.

Substituting (7) into (4), the system dynamics equation after joint torque feedback can be obtained:

$$M\left(q\right)\ddot{q}+C\left(q,\dot{q}\right)\dot{q}+g\left(q\right)=\tau+\tau_{\text{ext}} \tag{8}$$

$$B_\theta\ddot{\theta}+\tau+B_\theta B^{-1}\tau_f=u \tag{9}$$

After the manipulator grabs the power tool, it is hoped that the impedance behavior of the system in Cartesian coordinates can be expressed as the following relation through impedance control:

$$F=K_x\tilde{x}+D_x\dot{\tilde{x}} \tag{10}$$

Where, $F=\left(F_x,F_y,F_z,\tau_x,\tau_y,\tau_z\right)\in\mathbf{R}^{6\times 1}$ is the generalized contact force acting on the end of the manipulator; $\tilde{x}=x-x_s\in\mathbf{R}^{6\times 1}$ represents the generalized position coordinates of the three-dimensional space, that is, the difference between the actual stable position x at the end of the manipulator and the virtual desired position x_s at the end of the manipulator; $K_x\in\mathbf{R}^{6\times 6}$ represents the desired stiffness diagonal matrix; $D_x\in\mathbf{R}^{6\times 6}$ represents the desired damping diagonal matrix.

Since the actual control of the manipulator is performed in the joint space, it is necessary to convert the impedance relationship of (10) into the joint space.

Assume that the forward kinematics from joint space q to Cartesian space x are expressed as:

$$x=f\left(q\right) \tag{11}$$

Then, $\dot{x}=J(q)\dot{q}$. Since the impedance control law u in (9) is used to control the motor, if one uses the motor angle θ instead of the link side angles q in the forward kinematics [2], as shown by (12). The desired impedance behavior of the Cartesian space at the end of the manipulator expressed by (10) can be converted to the joint space by force Jacobian matrix, as shown by (13) and (14). It should be noted that x_s is a virtual desired position, which is a static set point, and its derivative is zero; $B_\theta B^{-1}\hat{\tau}_f$ is the friction torque compensation in control input.

$$\dot{x}=J(\theta)\dot{\theta} \tag{12}$$

$$u = B_\theta B^{-1} \hat{\tau}_f - J(\theta)^T (K_x \tilde{x}(\theta) + D_x \dot{x}) \quad (13)$$

$$\tilde{x}(\theta) = f(\theta) - x_s \quad (14)$$

Substituting (13) into (9), and regardless of the gravity term, the control model of the system can be expressed as:

$$M(q)\ddot{q} + C(q,\dot{q})\dot{q} = \tau + \tau_{ext} \quad (15)$$

$$B_\theta \ddot{\theta} + J(\theta)^T (K_x \tilde{x}(\theta) + D_x \dot{x}) + \tau + B_\theta B^{-1}(\tau_f - \hat{\tau}_f) = 0 \quad (16)$$

In (16), $B_\theta B^{-1}(\tau_f - \hat{\tau}_f)$ is the error between the estimated friction torque by identification and the actual friction torque.

B. Closed Loop System Stability Analysis

Considering that the screwing process can be divided into the free movement before the power tool contacts the bolt and the restricted movement of the screwing, in this paper, the stability of the closed-loop system is analyzed for these two processes.

1) Free movement before the power tool contacts the bolt:

Consider the following function $V(q,\dot{q},\theta,\dot{\theta})$ as a candidate Lyapunov function:

$$V(q,\dot{q},\theta,\dot{\theta}) = V_k + V_p + V_f \quad (17)$$

Herein V_k represents the kinetic part of the Lyapunov function and can be expressed as (18). Since the inertia matrix $M(q)$ and B_θ are both positive definite, the function V_k is positive definite with respect to $\dot{q}$ and $\dot{\theta}$. V_p represents the potential energy part of the Lyapunov function and can be expressed as (19). Since the joint stiffness diagonal matrix K and the Cartesian space desired stiffness diagonal matrix K_x are both positive definite, the function V_p is positive definite with respect to q and θ. V_f represents the energy term introduced by the friction compensation in the Lyapunov function, which can be expressed as (20), where $\tilde{\tau}_f = \tau_f - \hat{\tau}_f$ is the joint friction torque identification error vector, $Q = B_\theta B^{-1}$ is a constant value diagonal positive definite matrix, and the diagonal elements are positive.

$$V_k = \frac{1}{2}\dot{q}^T M(q)\dot{q} + \frac{1}{2}\dot{\theta}^T B_\theta \dot{\theta} \quad (18)$$

$$Vp = \frac{1}{2}(\theta - q)^T K(\theta - q) + \frac{1}{2}\tilde{x}(\theta)^T K_x \tilde{x}(\theta) \quad (19)$$

$$V_f = \tilde{\tau}_f^T Q \tilde{\tau}_f \quad (20)$$

Therefore, function (17) is a positive definite Lyapunov function.

After the manipulator grasps the power tool, the external force of the environment to the system is zero until the power tool contacts the bolt, that is, $\tau_{ext}=0$. At this time, along the system ((15), (16) and (5)), the derivative of $V(q,\dot{q},\theta,\dot{\theta})$ over time is as follows:

$$\dot{V}(q,\dot{q},\theta,\dot{\theta}) = -\dot{x}^T D_x \dot{x} + \dot{V}_f + \dot{\theta}^T Q \tilde{\tau}_f \quad (21)$$

First, consider the ideal case of accurate compensation of friction torque, $\tilde{\tau}_f = \tau_f - \hat{\tau}_f = 0$. Then (21) is simplified as:

$$\dot{V}(q,\dot{q},\theta,\dot{\theta}) = -\dot{x}^T D_x \dot{x} \quad (22)$$

Since the desired damping diagonal matrix D_x is positive definite, the system is stable at the equilibrium point. According to the principle of LaSalle, suppose $\dot{V} \equiv 0$, since D_x is a positive definite matrix, means $\dot{x} \equiv 0$, hence $\ddot{x} \equiv 0$. For the non-redundant degree of freedom manipulator studied in this paper, $J(\theta)$ is in a non-singular state during screwing operation, then $\dot{\theta} \equiv 0$. Therefore, the equilibrium point is globally asymptotic stable.

When there is an error between the friction torque identified and the actual friction torque, the friction compensation error is regarded as the disturbance of the system, and the following equation can be obtained:

$$\dot{V} = -\dot{x}^T D_x \dot{x} + \dot{\theta}^T Q \tilde{\tau}_f + \dot{V}_f \quad (23)$$

Input to State Stability(ISS) theorem: A control system is called input to state stable (ISS) [12]: there is a smooth positive definite upper limit function $V(e,t)$, a κ_∞ function γ_1, a κ function γ_2, making the following dissipative inequality valid:

$$\dot{V} \le -\gamma_1(|e|) + \gamma_2(|\zeta|) \quad (24)$$

Where e represents the system state error; ζ represents the disturbance input. Obviously, $\gamma_1(|\dot{x}|) = \dot{x}^T D_x \dot{x}$ is a κ_∞ function, $\gamma_2(|\tilde{\tau}_f|) = \mathrm{Max}(\dot{\theta}) \sum_1^6 Q_i |\tilde{\tau}_{f_i}| + 2\mathrm{Max}(\tilde{d}) \sum_1^6 Q_i |\tilde{\tau}_{f_i}|$ is a κ function.

The following relationship is valid:

$$\begin{aligned} \dot{V} &= -\dot{x}^T D_x \dot{x} + \dot{\theta}^T Q \tilde{\tau}_f + \dot{V}_f \\ &= -\dot{x}^T D_x \dot{x} + \sum_1^6 Q_i \dot{\theta}_i \tilde{\tau}_{f_i} + 2\sum_1^6 \tilde{d}_i Q_i \tilde{\tau}_{f_i} \\ &\le -\dot{x}^T D_x \dot{x} + \mathrm{Max}(\dot{\theta}) \sum_1^6 Q_i |\tilde{\tau}_{f_i}| + 2\mathrm{Max}(\tilde{d}) \sum_1^6 Q_i |\tilde{\tau}_{f_i}| \end{aligned} \quad (25)$$

Since the motor speed $\dot{\theta}$, the identification error of viscous friction coefficient $\tilde{d}$, and the identification error of friction torque $\tilde{\tau}_f$ are both bounded, the above formula satisfies the ISS condition, and it can be concluded that the closed-loop system with friction compensation is input to state stable.

2) Restricted movement of the screwing:

A system, input is u and output is y is said to be passive, if there is a continuously bounded energy storage function S that satisfies the following conditions:

$$\dot{S} \le u^T y \quad (26)$$

The closed-loop system (15) and (16) is considered as two subsystems, as shown in Fig. 5. Here, the contact process between the power tool and the screw is considered to be passive $(\dot{q} \to -\tau_{ext})$.

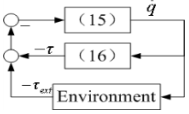

Fig. 5 System representation as interconnection of passive subsystems.

The passivity of rigid manipulator (15) has been proved very early, that is, $(\tau + \tau_{ext}) \to \dot{q}$ is passive. The storage function is selected:

$$S_q(q,\dot{q}) = \frac{1}{2}\dot{q}^T M(q)\dot{q} \quad (27)$$

The derivative of (27) along the system (15) can be expressed as:

$$\dot{S}_q(q,\dot{q}) = \dot{q}^T(\tau + \tau_{ext}) \quad (28)$$

Similarly, the passivity of (16) $(\dot{q} \to -\tau)$ can be shown with the storage function:

$$S_\theta(q,\theta,\dot{\theta}) = \frac{1}{2}\dot{\theta}^T B_\theta \dot{\theta} + \frac{1}{2}(\theta - q)^T K(\theta - q) + \frac{1}{2}\tilde{x}(\theta)^T K_x \tilde{x}(\theta) \quad (29)$$

Considering the ideal case of accurate compensation of friction torque, the derivative of (29) along the system (16) is obtained:

$$\dot{S}_\theta(q,\theta,\dot{\theta}) = -\dot{x}^T D_x \dot{x} - \dot{q}^T \tau \tag{30}$$

Therefore, the closed loop system formed by the feedback connection of the passive subsystem (15) and (16) is also passive. Even if the friction torque is not accurately compensated, it can be seen from the on-orbit identification results that the area enclosed by the identification curve and the $\dot{\theta}$ axis is smaller than the area enclosed by the actual measurement value and the $\dot{\theta}$ axis [11]. The energy injected into the system caused by the inaccurate friction torque identification tends to dissipate. Therefore, the system remains passive.

In summary, theoretical analysis shows that:

- After the control mode is switched to impedance control, until the power tool comes into contact with the screw, the movement of the manipulator to the set point is asymptotically stable.
- During the contact process between power tool and bolt, the system is passive. The collision between the power tool and the screw will not cause the control system to diverge. And by properly selecting the impedance parameters, the force between the power tool and the screw can be controlled within 40N. This part is further verified in Section V.

C. *Impedance Parameters Design*

According to Hogan[1], for the task in contact with a rigid environment, the impedance of the end point of the manipulator is like a soft spring to ensure the contact stability. The stiffness of the workbench is about 2×10^4N/m. First, set the Cartesian stiffness parameters as shown in Table I, and then use the double diagonalization design method [3] to design the Cartesian damping parameters.

TABLE I
IMPEDANCE PARAMETERS

Direction	Position(N/m)			Orientation(Nm/rad)		
	x	*y*	*z*	*rx*	*ry*	*rz*
Stiffness	500	1000	1000	100	100	100

According to the three-dimensional model Fig. 1, the nominal contact position between the end of the power tool and the top of the bolt is –369 mm in coordinate system O_bXYZ. In the screwing phase, the desired position of the manipulator in the X direction is –375 mm. Considering the static condition $\dot{\tilde{x}} \cong 0$, the contact force F_x between the manipulator and the workbench is maintained at about 3N.

Referring to the results of the stiffness analysis of the workbench in Section II, the contact force is much less than 40N, which can ensure that the tolerance is always greater than the system error, and the bolt will not come out. Therefore, the parameters can meet the mission requirements.

V. VERIFICATION

A. *Simulation*

The dynamic model of the manipulator system (including the contact dynamic model of the power tool and the bolt) is established in ADAMS, and the Matlab module is generated. The system control model is built in Matlab for simulation, as shown in Fig. 6.

Fig. 7 shows the desired inputs and the Cartesian space simulation results for the end of the manipulator system during the power tool inserting the bolt hole and screwing. During the 267s~272s, the control mode is switched from visual servoing control to impedance control, and the manipulator drives the power tool to be inserted along the X direction of the coordinate system O_bXYZ. From the simulation curves, it can be seen that the mode switching achieves a smooth transition. The position error between the simulation result and the reference input does not exceed ±0.5 mm, and the angular error does not exceed ±0.5°. Starting from 272s, the power tool is inserted into the bolt hole along the X direction, and the power tool is inserted into the lowest point of the bolt hole around 277s.

It can be seen from Fig. 8 that the force along the X direction is well controlled under impedance control. During screwing, the contact force does not exceed 3N, which meets the requirement of contact force less than 40N. The control effect and design are well matched.

The simulation results show that the proposed control strategy can better meet the mission requirements.

B. *On-orbit Experiment*

In the orbital experiment, using the impedance control strategy discussed, the manipulator accurately inserts the power tool into the bolt hole and loosens the bolt successfully, as shown in Fig. 9. By analyzing the telemetry parameters of on-orbit experiment, the Cartesian position and orientation of the manipulator are basically the same as the simulation results. Compared with the on-orbit data, the simulation error of the Cartesian force / torque at the end of the manipulator is within 10%.

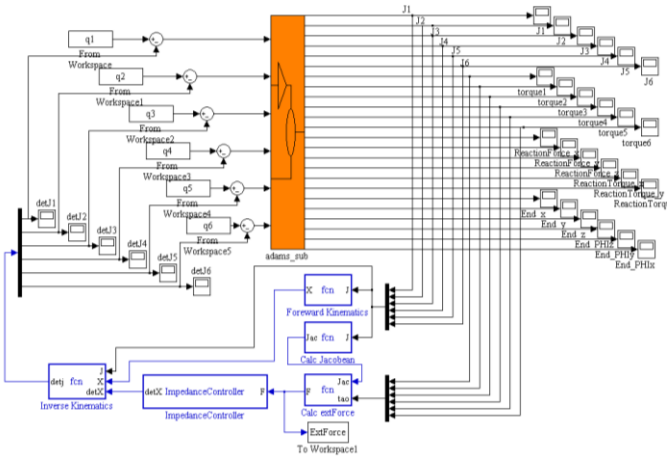

Fig. 6 Simulation model.

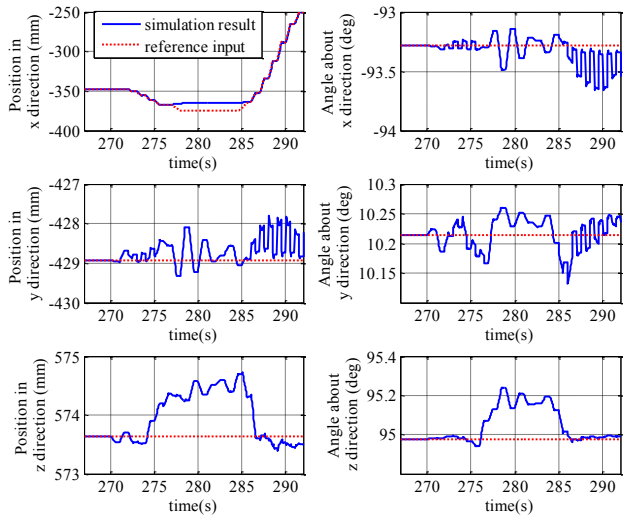

Fig. 7 Cartesian position and orientation of manipulator during screwing.

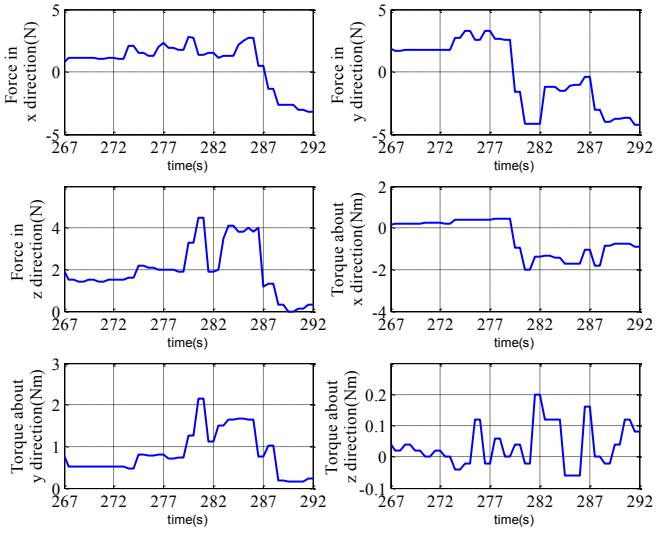

Fig. 8 Cartesian force/torque simulation results of manipulator during screwing.

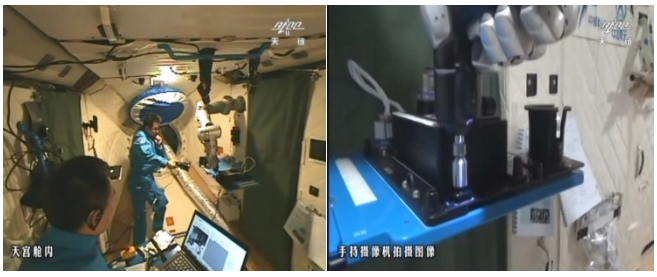

Fig. 9 Manipulator system on-orbit experiment.

VI. Conclusion

In this paper, a Cartesian impedance control strategy based on friction torque compensation is proposed for the mission requirements of the space manipulator screwing. Through reasonable parameters selection, the strategy successfully realizes the accurate positioning and controls the contact force within 3N, and finally meets the predetermined design requirements.

It is worth noting that the scheme requires accurate models and parameters of the friction torque before the mission is executed. Therefore, the identification accuracy of the on-orbit friction torque becomes the decisive factor that restricts the control accuracy of the method.

Acknowledgment

This work is partially supported by National Natural Science Foundation of China(Grant No. 51521003, 61803124).

References

[1] N. Hogan, “Impedance control: an approach to manipulation: Part I-III,” *ASME Journal of Dynamic System, Measurement and Control*, vol. 107, pp. 1–24, March 1985.

[2] C.Ott, A.Albu-Schaeffer, A.Kugiy, et al, “A passivity based Cartesian impedance controller for flexible joint robots Part I: torque feedback and gravity compensation,” in *Proceedings of the 2004 IEEE International Conference on Robotics and Automation*, New Orleans, 2004, pp. 2659–2665.

[3] A.Albu-Schaeffer, C.Ott, G. Hirzinger, “A passivity based Cartesian impedance controller for flexible joint robots part II: full state feedback, impedance design and experiments,” in *Proceedings of the 2004 IEEE International Conference on Robotics and Automation*, New Orleans, 2004, pp. 2666–2672.

[4] Z. P. Chen, N. Y. Lii, T. Wimboeck, S. W. Fan and H. Liu, “Experimental evaluation of Cartesian and joint impedance control with adaptive friction compensation for the dexterous robot hand DLR-HIT II,” *International Journal of Humanoid Robots*, vol. 8, pp. 649–671, 2011.

[5] K. Landzettel, C. Preusche, A. Albu-Schaffer, D. Reintsema, B. Rebele, and G. Hirzinger, “Robotic on-orbit servicing - DLR's experience and perspective,” in *Proceedings of the 2006 IEEE/RSJ International Conference on Intelligent Robots and Systems*, Beijing, 2006, pp. 4587–4594.

[6] M. A. Diftler, J. S. Mehling, et al, “Robonaut 2 – The first humanoid robot in space,” in *Proceedings of the 2011 IEEE International Conference on Robotics and Automation*, Shanghai, 2011, pp. 2178–2183.

[7] M. Oda, “Space robot experiments on NASDA's ETS-VII satellite-preliminary overview of the experiment results,” in *Proceedings of the 1999 IEEE International Conference on Robotics and Automation*, Detroit, 1999, pp. 1390–1395.

[8] H. Liu, Y.C. Liu, M.H. Jin, K. Sun and J. B. Huang, “An experimental study on Cartesian impedance control for a joint torque-based manipulator,” *Advanced Robotics*, vol. 22, pp. 1155–1180, Nov. 2008.

[9] J. B. Huang, Z. W. Xie, H. Liu and K. Sun. “Adaptive Cartesian impedance control system for flexible joint robot by using DSP/FPGA architecture,” *International Journal of Robotics and Automation*, vol. 23, pp. 271–278, 2008.

[10] D. Y. Liu, H. Liu, Y. He, B. N. Zhang, Y. C. Liu, Z. Q. Li, C. Luo, “Research on flexible joint friction identification of space lab manipulator,” in *Proceedings of the 2018 IEEE International Conference on Mechatronics and Automation*, Changchun, 2018, pp. 614–619.

[11] D. Y. Liu, H. Liu, Y. He, B. N. Zhang, Z. Q. Li, M. H. Jin, “Visual servoing control strategy for on-orbit servicing of space manipulator system,” *Robot*, vol. 40, pp. 742–749, Sep. 2018.

[12] H. Khalil, J. Grizzle, *Nonlinear systems*. New Jersey, USA: Prentice hall, 1992, pp. 131–147.